

Spin Alignment, Phase Transition and Neutral Pseudoscalar Meson Dynamics of QGP in the Presences of Magnetic and Vorticity Fields

- 1. The Spin Alignment and Phase Structure of Thermal QGP under Rotation**
- 2. The Anomalous Magnetic Moment and Pseudoscalar Meson Dynamics in the Magnetized QCD Background**
- 3. Summary and Conclusions**

Sheng-Qin Feng (冯笙琴) (Three Gorges Univ.)

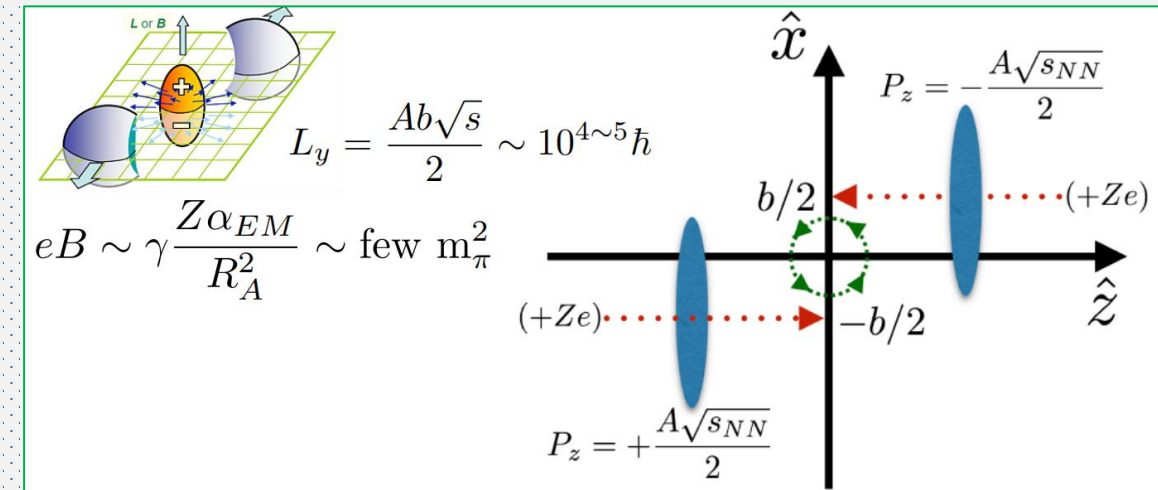
Based on:

- (1) Yang Hua and Sheng-Qin Feng, Phys. Rev. D **111**, 036012 (2025);**
- (2) C.-Y. Yang and S.-Q. Feng, Phys. Rev. D **112**, 036008 (2025) ;**
- (3) Y.-W. Qiu and S.-Q. Feng, Phys. Rev. D **107**, 076004 (2023);**
- (4) X.-Q. Zhu and S.-Q. Feng, Phys. Rev. D **107**, 016018 (2023);**
- (5) Y.-W. Qiu and S.-Q. Feng, X.-Q. Zhu, Phys. Rev. D **108**, 116022 (2023).**

The 26th international symposium on spin physics (SPIN2025) , Qingdao, Sept. 21 - 26, 2025

Extremal Vorticity and Magnetic Fields in Relativistic HIC

For non-central high-energy collisions, the dense matter produced in the overlapped region of the collision will carry a global angular momentum along the direction opposite to the reaction plane ($-\hat{y}$). Assuming that a partonic system is formed immediately following the initial collision, interactions among produced partons will lead to formation of a quark – gluon plasma (QGP).



Vorticity fields $\omega \sim 10^{21} s^{-1}$

STAR, Nature 548 (2017) 62-65;

Becattini, Liao, Lisa,

Lect.Notes Phys. 987 (2021).

Magnetic fields $B \sim 10^{18} \text{ Gauss}$

W. T. Deng, X. G. Huang,

PRC 85, 044907 (2012).

QCD

Phase structure

Spin polarization

Jet quenching

Meson/baryon mass

⋮

NJL model

Quark meson model

Lattice QCD

Holographic model

⋮

The 26th international symposium on spin physics (SPIN2025), Qingdao, Sept. 21 - 26, 2025

1. The Spin Alignment and Phase Structure of Thermal QGP under Rotation

- (1) Yang Hua and Sheng-Qin Feng, Phys. Rev. D **111**, 036012 (2025);
- (2) Yan-Ru Bao and Sheng-Qin Feng, Phys. Rev. D **109**, 096033 (2024).

From Gluon Topology to Quark Chirality

$$Q_w = \frac{1}{32\pi^2} \int d^4x F^{a\mu\nu} \tilde{F}_{\mu\nu}^a$$

In the quark–gluon plasma (QGP), once these gluon configurations are excited at a certain spacetime point, the topological charge of the vacuum around that point will be altered by these gluon configurations. The chirality imbalance $N_5 = N_R - N_L = -2Q_w$ is induced by the nonzero topological charge through the axial anomaly of QCD.

A non-zero Q_w will induce a corresponding fluctuation in the quark chiral imbalance N_5 . **This process will result in chiral imbalance between right and left quarks, leading to the violation of parity (P) and charge-parity (CP) symmetry in the thermal plasma.**

The effects of a chiral imbalance in a medium can be implemented in the grand canonical ensemble by introducing a chiral chemical potential μ_5 .

The Lagrangian of NJL model with the chiral chemical potential μ_5

The QCD matter produced in heavy-ion non-central collisions can rotate rapidly with local angular velocities ranging from 0.01 to 0.1 GeV. **The Lagrangian of two flavors under the mean field approximation of the NJL model is given**

chiral imbalance

Orbital motion

Spin motion

$$\mathcal{L}_{MFA} = \bar{\psi} \left[i\gamma^\mu \partial_\mu - M + \mu\gamma^0 + \mu_5 \gamma^0 \gamma^5 + (\gamma^0)^{-1} \left((\vec{\omega} \times \vec{x}) \cdot (-i\vec{\partial}) + \vec{\omega} \cdot \vec{S}_{4 \times 4} \right) \right] - G_s \sigma^2$$

In cylindrical coordinates, the general positive-energy solutions for the quark field from the Dirac equation corresponding to the above Lagrangian is given as

Reference:

- (1). Y. Jiang and J. Liao, Phys. Rev. Lett. 117, 192302 (2016);
- (2). Yang Hua and Sheng-Qin Feng, Phys. Rev. D 111, 036012 (2025)

$$\psi(\theta, r) = e^{-iEt + iP_z z} \begin{pmatrix} ce^{in\theta} J_n(p_t r) \\ ide^{i(n+1)\theta} J_{n+1}(p_t r) \\ c'e^{in\theta} J_n(p_t r) \\ id'e^{i(n+1)\theta} J_{n+1}(p_t r) \end{pmatrix}$$

The energy level, thermodynamic potential and chiral charge density

Through the calculation of the finite temperature field, the energy level and thermodynamic potential by rotation are obtained as follows:

$$E_{n,s} = \sqrt{\left(\sqrt{p_t^2 + p_z^2} - s\mu_5\right)^2 + M^2} - \left(n + \frac{1}{2}\right)\omega$$

$$\Omega = \frac{(M - m)^2}{4G_s} - \frac{N_f N_c}{8\pi^2} \sum_{n=-\infty}^{+\infty} \sum_{s=\pm 1} \int dp_t^2 dp_z W_{n,s} \left\{ E_{n,s} + T \ln \left[1 + e^{-\beta(E_{n,s} - u)} \right] + T \ln \left[1 + e^{-\beta(E_{n,s} + u)} \right] \right\}$$

$$W_{n,s} = \left[J_n^2(p_t r) + \lambda^2 J_{n+1}^2(p_t r) \right] / (1 + \lambda^2)$$

Gap equation: $\frac{\partial \Omega}{\partial M} = 0, \quad \frac{\partial^2 \Omega}{\partial M^2} > 0$

The chiral charge density n_5 is defined by : $n_5 = -\frac{\partial \Omega}{\partial \mu_5}$

Spin Alignment of ρ Mesons

The ρ meson is a vector meson composed of a quark and an antiquark with parallel spins (total spin $s = 1$). In extreme environments such as the rotating quark-gluon plasma (QGP) produced in non-central heavy-ion collisions, ρ mesons may exhibit spin alignment — a phenomenon where their spin states correlate with the direction of system rotation.

The key observable for studying spin alignment is the spin density matrix element ρ_{00} , which describes the probability of the meson being in the spin states $s_z = 0$. In the absence of polarization, $\rho_{00} = 1/3$ indicating isotropic spin distribution. A deviation from 1/3 signals spin polarization along a specific direction.

Spin Alignment of ρ Mesons

The spin alignment ρ_{00} is derived using a quark recombination model, where polarized quarks and antiquarks combine to form ρ mesons:

$$\rho_{00} = \frac{1 - P_q P_{\bar{q}}}{3 + P_q P_{\bar{q}}} \approx \frac{1}{3} - \frac{4}{9} P_q P_{\bar{q}}$$

P_q and $P_{\bar{q}}$ are the polarization of quarks and antiquarks, respectively.

- [1] Z.-T. Liang and X.-N. Wang, Phys. Rev. Lett. **94**, 102301 (2005);
- [2] Z.-T. Liang and X.-N. Wang, Phys. Lett. **B 629**, 20 (2005).

The 26th international symposium on spin physics (SPIN2025) , Qingdao, Sept. 21 - 26, 2025



Related theory

According to the **quark recombination model** [1, 2], the spin alignment of fermions is composed of the particle number densities of quarks and antiquarks, which is given by the partial derivative of the thermodynamic potential with respect to the chemical potential:

$$N_{\uparrow}^{+} = \frac{N_f N_c}{4\pi^2} \sum_{n=-\infty}^{+\infty} \sum_{s=\pm 1} \int dp_t dp_z p_t \frac{J_n^2(p_t r)}{1 + \lambda^2} \frac{e^{-\beta(E_{n,s} - \mu)}}{1 + e^{-\beta(E_{n,s} - \mu)}}$$

$$N_{\downarrow}^{+} = \frac{N_f N_c}{4\pi^2} \sum_{n=-\infty}^{+\infty} \sum_{s=\pm 1} \int dp_t dp_z p_t \frac{\lambda^2 J_{n+1}^2(p_t r)}{1 + \lambda^2} \frac{e^{-\beta(E_{n,s} - \mu)}}{1 + e^{-\beta(E_{n,s} - \mu)}}$$

$$N_{\uparrow}^{-} = -\frac{N_f N_c}{4\pi^2} \sum_{n=-\infty}^{+\infty} \sum_{s=\pm 1} \int dp_t dp_z p_t \frac{J_n^2(p_t r)}{1 + \lambda^2} \frac{e^{-\beta(E_{n,s} + \mu)}}{1 + e^{-\beta(E_{n,s} + \mu)}}$$

$$N_{\downarrow}^{-} = -\frac{N_f N_c}{4\pi^2} \sum_{n=-\infty}^{+\infty} \sum_{s=\pm 1} \int dp_t dp_z p_t \frac{\lambda^2 J_{n+1}^2(p_t r)}{1 + \lambda^2} \frac{e^{-\beta(E_{n,s} + \mu)}}{1 + e^{-\beta(E_{n,s} + \mu)}}$$

The 26th international symposium on spin physics (SPIN2025) , Qingdao, Sept. 21 - 26, 2025



Comparisons with other model

When studying the spin alignment of vector mesons ρ , besides our quark recombination model, there is also the **quark condensation model** [1]. The spin alignment corresponding to vector mesons ρ can take the following form

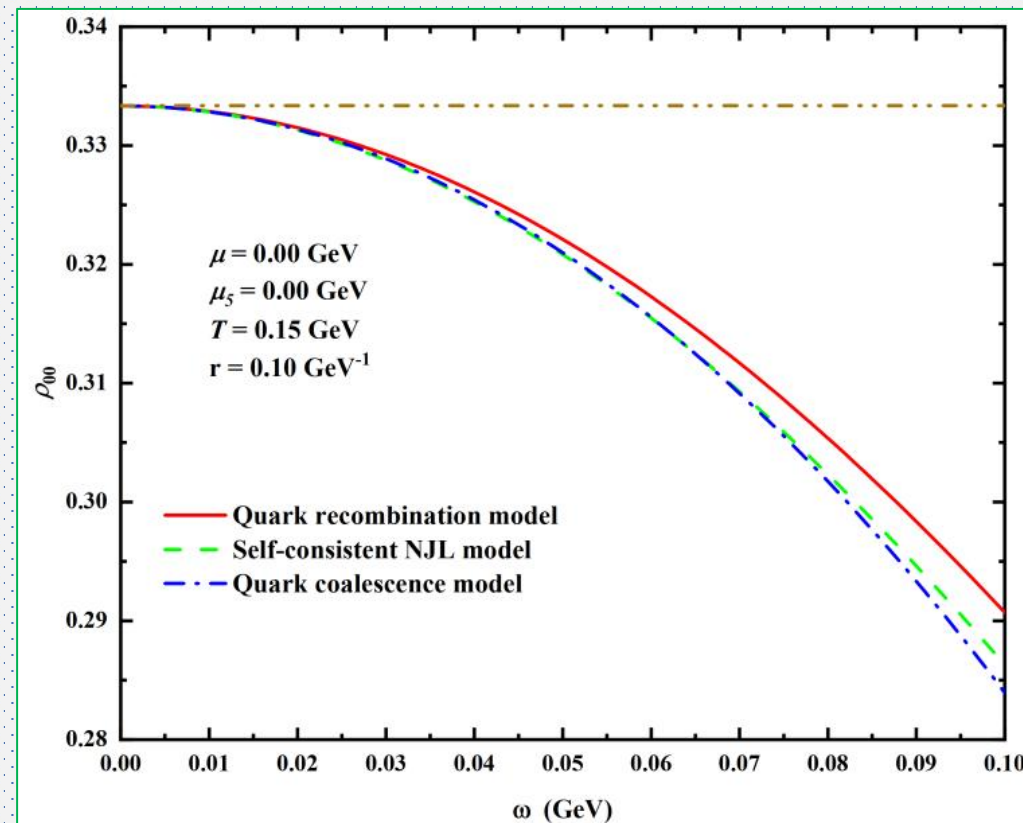
$$\rho_{00} = \frac{1}{3} - \frac{4}{9}(\beta\omega)^2$$

Another spin polarization model is **self-consistent NJL model** [2], the spin alignment of vector mesons (including ρ and ϕ) ($T = 150$ MeV), exhibits the following relationship:

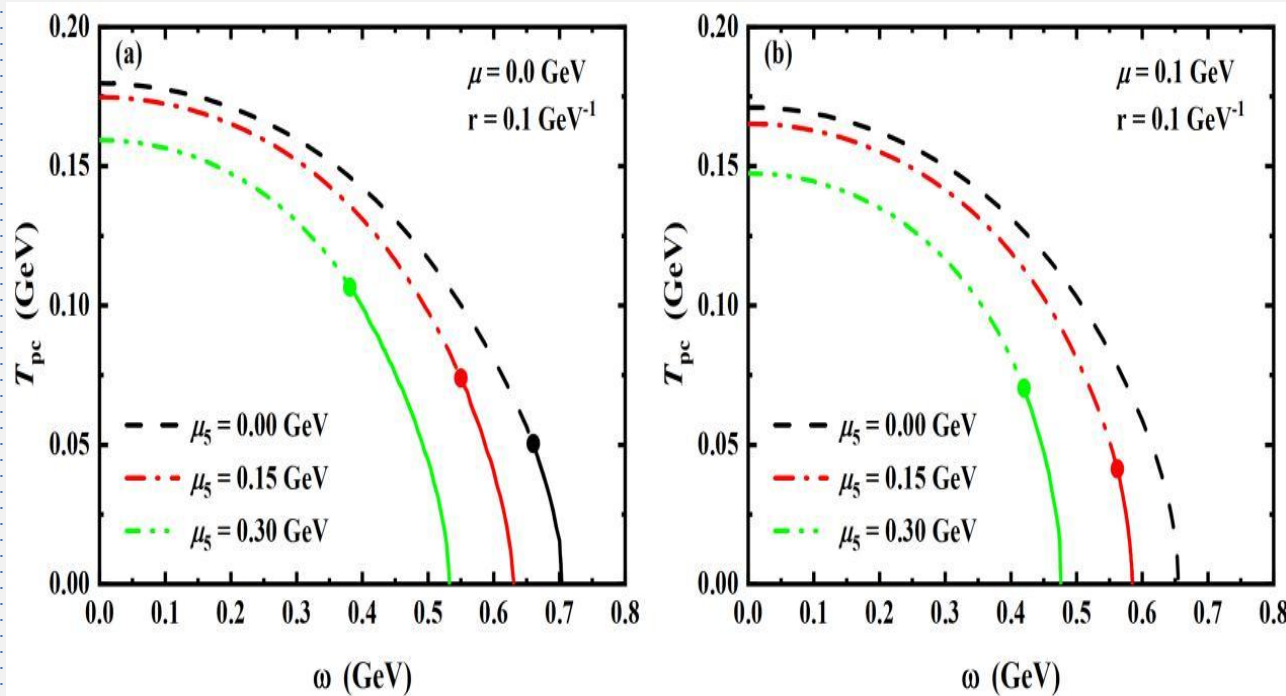
$$\rho_{00} = \frac{1}{3} - 5.10\omega^2 + 39.62\omega^4$$

[1] Y.-G. Yang, R.-H. Fang, Q. Wang, and X.-N. Wang, Phys. Rev. C **97**, 034917(2018).

[2] M. Wei and M. Huang, Chin. Phys. C **47**, 104105(2023).



The phase structure of $T - \omega$ plane with chiral chemical potential



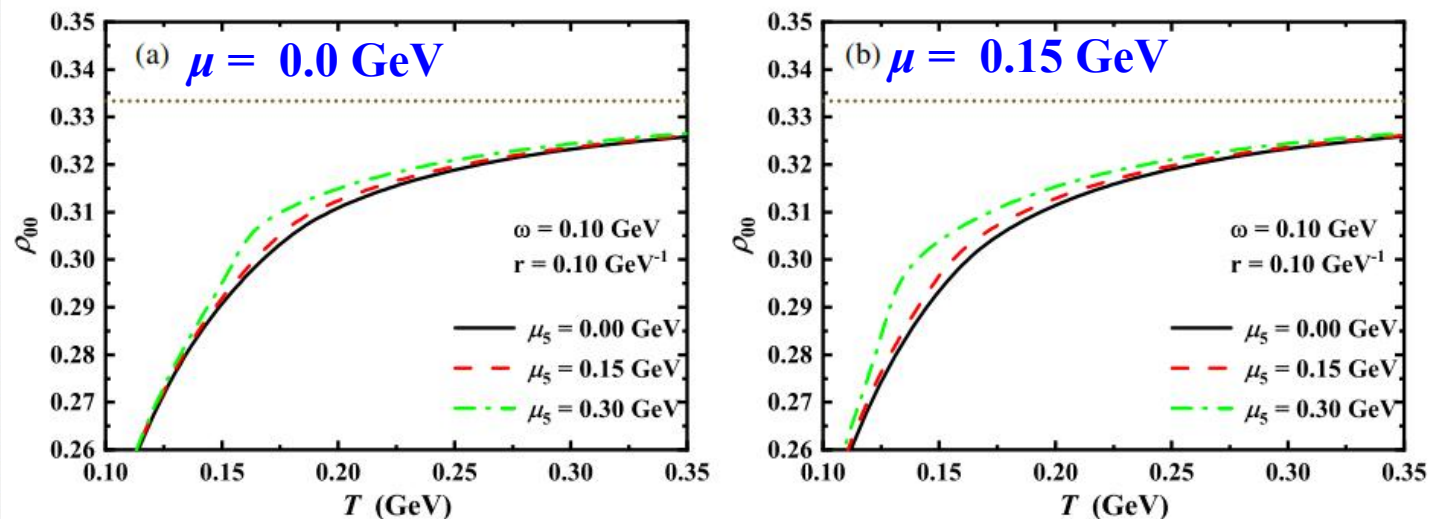
This figure illustrates the chiral phase diagram in the $T_{pc} - \omega$ plane for varying chiral chemical potentials μ_5 . **The critical temperature T_{pc} decreases with increasing μ_5 , but the critical end point (CEP) shifts toward higher T and lower ω .**

This is the first study to systematically explore how chiral imbalance (via μ_5) modifies the phase structure of a rotating QCD medium. **It uniquely demonstrates that μ_5 suppresses T_{pc} while enhancing the CEP temperature, revealing a competition between rotation and chiral imbalance.**

Y. Hua and S.-Q. Feng, Phys. Rev. D **111**, 036012 (2025).

It resolves how **chiral imbalance** alters the order and criticality of the chiral phase transition under rotation, providing insights into **the interplay of vorticity and parity violation in quark-gluon plasma (QGP).**

The relationship between spin alignment ρ_{00} and temperature T



Research Content: ρ_{00} approaches 1/3 (isotropic spin alignment) at high T , while deviating near the phase transition temperature.

Increasing μ_5 enhances ρ_{00} , reducing spin polarization.

Innovation & Impact: This is the first work to connect chiral imbalance (μ_5) with vector meson spin alignment, **showing that μ_5 counteracts rotation-induced polarization near T_{pc} .**

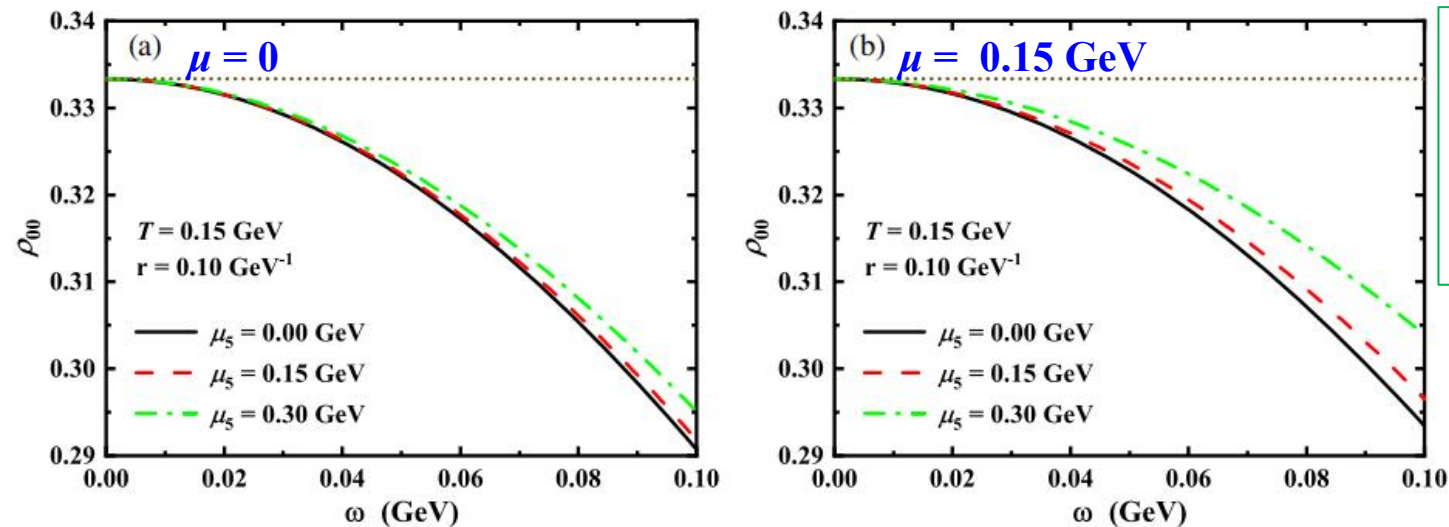
Spin alignment ρ_{00} of ρ mesons as a function of temperature T

Key Problem Solved: It explains how chiral imbalance moderates spin polarization in a temperature-dependent manner, crucial for interpreting experimental ρ_{00} data in QGP.

- (1) Z.-T. Liang and X.-N. Wang, Phys. Rev. Lett. 94, 102301 (2005);
- (2) Z.-T. Liang and X.-N. Wang, Phys. Lett. B 629, 20 (2005);
- (3) Y. Hua and S.-Q. Feng, Phys. Rev. D 111, 036012 (2025).

The 26th international symposium on spin physics (SPIN2025), Qingdao, Sept. 21 - 26, 2025

The relationship between spin alignment ρ_{00} and rotational velocity ω



Research Content: ρ_{00} decreases with ω , deviating from $1/3$ (indicating polarization). Larger μ_5 reduces this deviation, particularly at high ω .

Innovation & Impact: It demonstrates that **chiral imbalance suppresses rotation-induced spin polarization**, offering a mechanism to tune meson spin states via μ_5

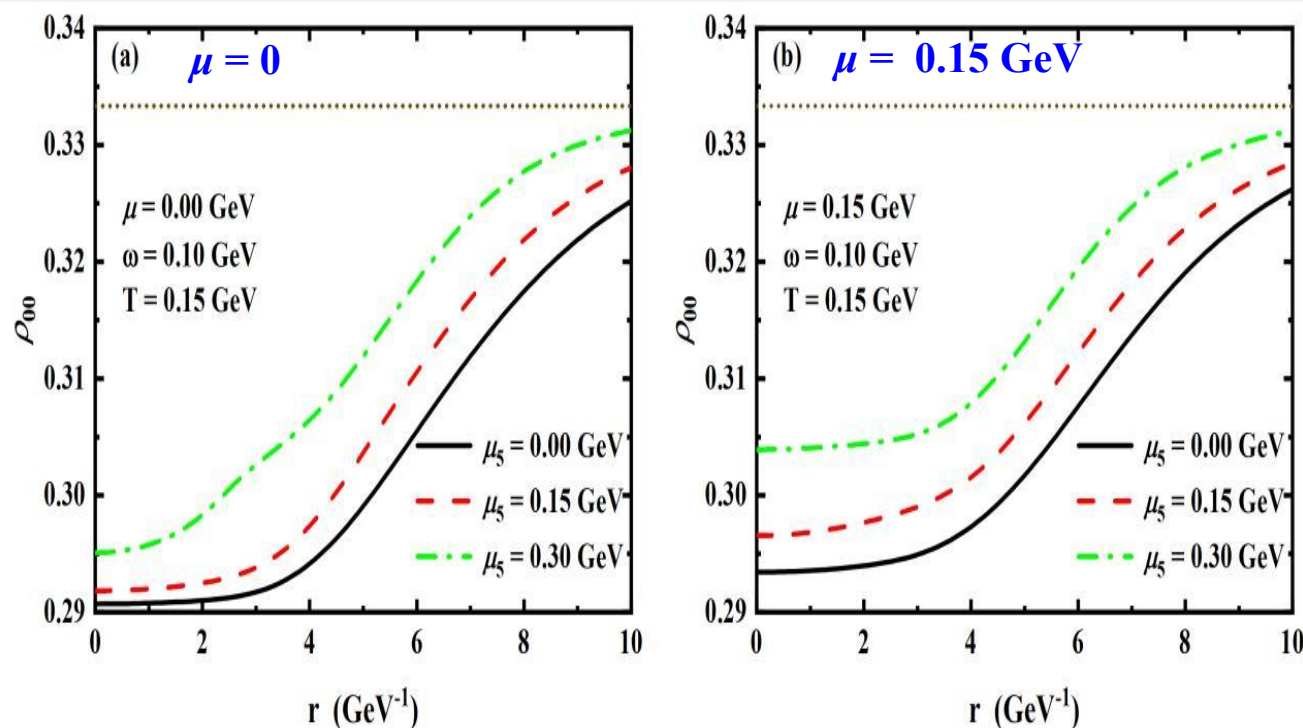
Spin alignment ρ_{00} of ρ mesons as a function of ω

Key Problem Solved: It resolves how competing effects of rotation and **chiral imbalance** determine the net polarization of vector mesons, vital for probing spin-orbit coupling in QCD matter.

Y. Hua and S.-Q. Feng, Phys. Rev. **D 111**, 036012 (2025)

The 26th international symposium on spin physics (SPIN2025) , Qingdao, Sept. 21 - 26, 2025

The relationship between spin alignment ρ_{00} and rotational velocity ω



Research Content: ρ_{00} increases with r , approaching $1/3$, showing reduced polarization away from the rotation center. μ_5 enhances ρ_{00} at all r , especially near T_{pc} .

Innovation & Impact: This study pioneers the spatial analysis of spin alignment in rotating systems, revealing radial gradients in polarization and the moderating role of μ_5 .

Key Problem Solved: It identifies the spatial inhomogeneity of spin polarization in vortical QGP, essential for understanding local spin dynamics in finite-size systems like heavy-ion collisions.

Spin alignment ρ_{00} of ρ mesons as a function of radius r

Y. Hua and S.-Q. Feng, Phys. Rev. **D 111**, 036012 (2025).

The 26th international symposium on spin physics (SPIN2025) , Qinddao, Sept. 21 - 26, 2025

2. Anomalous Magnetic Moment (AMM) and Neutral Pseudoscalar Meson Dynamics in Magnetized QCD Matter

- (1) C.-Y. Yang and S.-Q. Feng, Phys. Rev. D **112**, 036008 (2025);
- (2) X.-Q. Zhu and S.-Q. Feng, Phys. Rev. D **107**, 016018 (2023);
- (3) Y.-W. Qiu and S.-Q. Feng, X.-Q. Zhu, Phys. Rev. D **108**, 116022 (2023)

The 26th international symposium on spin physics (SPIN2025) , Qingdao, Sept. 21 - 26, 2025

The SU(3) NJL model with quark anomalous magnetic moment (AMM)

Lagrangian density (**three flavors, broken isospin symmetry**)

Landau gauge $A_\mu = (0, 0, xB, 0)$

$$\mathcal{L}_{NJL} = \sum_{f=u,d,s} \bar{\psi}_f (i\gamma^\mu D_\mu^{(f)} - m_f - \frac{1}{2} e_f \kappa_f \sigma^{\mu\nu} F_{\mu\nu}) \psi_f + \\ G \sum_{a=0}^8 [(\bar{\psi} \lambda_a \psi)^2 + (\bar{\psi} i\gamma^5 \lambda_a \psi)^2] - K(\det[\bar{\psi}(1 + \gamma^5)\psi] + \det[\bar{\psi}(1 - \gamma^5)\psi])$$

M. Strickland et.al., PRD 86, 125032 (2012).

The contribution of the AMM to the Lagrangian density does arise from the interaction between the AMM and the quark spin.

In the NJL Lagrangian, the AMM term is:

$$-\frac{1}{2} e_f \kappa_f \sigma^{\mu\nu} F_{\mu\nu}$$

where:

- $\sigma^{\mu\nu} = \frac{i}{2} [\gamma^\mu, \gamma^\nu]$ is the spin tensor,
- $F_{\mu\nu}$ is the electromagnetic field tensor,
- κ_f is the quark AMM.

Thus, the AMM explicitly introduces a **spin-magnetic field interaction** into the Lagrangian, influencing quark dynamics, chiral symmetry breaking, and meson properties in a magnetic environment.

The 26th international symposium on spin physics (SPIN2025) , Qingdao, Sept. 21 - 26, 2025

The SU(3) NJL model with quark AMM

Mean-field approximation:

Thermodynamic potential:

$$\Omega_{MF} = \Omega_q + 2G(\sigma_u^2 + \sigma_d^2 + \sigma_s^2) - 4K\sigma_u\sigma_d\sigma_s$$

where:
$$\Omega_q = -3 \sum_{f=u,d,s} \frac{|q_f B|}{2\pi} \sum_n \sum_{s=\pm 1} \int \frac{dp_z}{2\pi} \left[E_{fns} + T \ln \left(1 + e^{-\frac{E_{fns} + \mu}{T}} \right) + T \ln \left(1 + e^{-\frac{E_{fns} - \mu}{T}} \right) \right]$$

Gap eqs: $\partial\Omega_{MF}/\partial\sigma_f = 0 \longrightarrow M_f = m_f - 4G\sigma_f + 2K \prod_{f'=f} \sigma_{f'}$

minimizing: Ω_{MF}

Chiral condensates:
$$\sigma_f = \langle \bar{\psi}_f \psi_f \rangle = -\frac{|e_f B|}{(2\pi)^2} \int dp_z \sum_{n,s} \frac{M_f}{E_{fns}} \left(1 - \frac{s\kappa_f e_f B}{M_{nf}} \right) \left(1 - \frac{1}{e^{(E_{fns}-\mu)/T} + 1} - \frac{1}{e^{(E_{fns}+\mu)/T} + 1} \right)$$

Energy eigenvalue:

$$E_{fns} = \sqrt{p_z^2 + (\underbrace{M_{nf}}_{\text{AMM}} - s\kappa_f e_f B)^2}, \quad M_{nf} = \sqrt{M_f^2 + 2n|e_f B|}$$

AMM

The 26th international symposium on spin physics (SPIN2025) , Qingdao, Sept. 21 - 26, 2025

The SU(3) NJL model with quark AMM

Transforming the six-fermion interaction into an effective four-fermion

➤ interaction, one obtains:

$$\begin{aligned}\mathcal{L}_{NJL} = & \sum_{f=u,d,s} \bar{\psi}_f (i\gamma^\mu D_\mu^{(f)} - m_f - \frac{1}{2} e_f \kappa_f \sigma^{\mu\nu} F_{\mu\nu}) \psi_f \\ & + \sum_{a=0}^8 [K_a^- (\bar{\psi} \lambda_a \psi)^2 + K_a^+ (\bar{\psi} i\gamma^5 \lambda_a \psi)^2] \\ & + K_{30}^- (\bar{\psi} \lambda_3 \psi) (\bar{\psi} \lambda_0 \psi) + K_{30}^+ (\bar{\psi} i\gamma^5 \lambda_3 \psi) (\bar{\psi} i\gamma^5 \lambda_0 \psi) \\ & + K_{80}^- (\bar{\psi} \lambda_8 \psi) (\bar{\psi} \lambda_0 \psi) + K_{80}^+ (\bar{\psi} i\gamma^5 \lambda_8 \psi) (\bar{\psi} i\gamma^5 \lambda_0 \psi) \\ & + K_{83}^- (\bar{\psi} \lambda_8 \psi) (\bar{\psi} \lambda_3 \psi) + K_{83}^+ (\bar{\psi} i\gamma^5 \lambda_8 \psi) (\bar{\psi} i\gamma^5 \lambda_3 \psi) \\ & + K_{03}^- (\bar{\psi} \lambda_0 \psi) (\bar{\psi} \lambda_3 \psi) + K_{03}^+ (\bar{\psi} i\gamma^5 \lambda_0 \psi) (\bar{\psi} i\gamma^5 \lambda_3 \psi) \\ & + K_{08}^- (\bar{\psi} \lambda_0 \psi) (\bar{\psi} \lambda_8 \psi) + K_{08}^+ (\bar{\psi} i\gamma^5 \lambda_0 \psi) (\bar{\psi} i\gamma^5 \lambda_8 \psi) \\ & + K_{38}^- (\bar{\psi} \lambda_3 \psi) (\bar{\psi} \lambda_8 \psi) + K_{38}^+ (\bar{\psi} i\gamma^5 \lambda_3 \psi) (\bar{\psi} i\gamma^5 \lambda_8 \psi)\end{aligned}$$

Effective coupling constants:

$$K_0^\pm = G \pm \frac{1}{3} K (\sigma_u + \sigma_d + \sigma_s),$$

$$K_1^\pm = K_2^\pm = K_3^\pm = G \pm \frac{1}{2} K \sigma_s,$$

$$K_4^\pm = K_5^\pm = G \pm \frac{1}{2} K \sigma_d,$$

$$K_6^\pm = K_7^\pm = G \pm \frac{1}{2} K \sigma_u,$$

$$K_8^\pm = G \pm \frac{1}{6} K (2\sigma_u + 2\sigma_d - \sigma_s),$$

$$K_{30}^\pm = K_{03}^\pm = \mp \frac{1}{2\sqrt{6}} K (\sigma_u - \sigma_d),$$

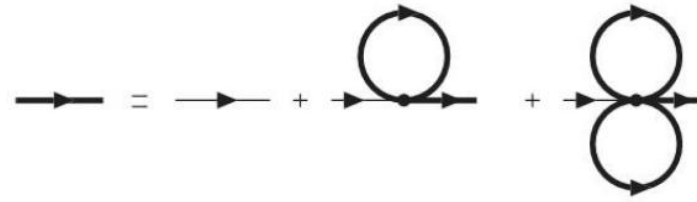
$$K_{80}^\pm = K_{08}^\pm = \pm \frac{\sqrt{2}}{12} K (\sigma_u + \sigma_d - 2\sigma_s),$$

$$K_{83}^\pm = K_{38}^\pm = \pm \frac{1}{2\sqrt{3}} K (\sigma_u - \sigma_d),$$

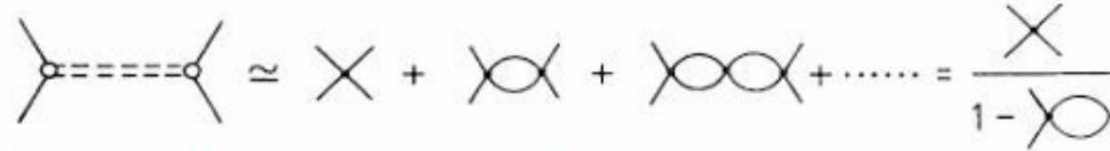
➤ **Chiral condensates:** $\sigma_u = \langle \bar{\psi}_u \psi_u \rangle, \sigma_d = \langle \bar{\psi}_d \psi_d \rangle, \sigma_s = \langle \bar{\psi}_s \psi_s \rangle$

➤ Ideas:

(1) Quarks: mean-field



(2) Mesons: RPA resummation (quantum fluctuation)



S. Klevansky, Rev. Mod. Phys. 64, 649 (1992).
M. Buballa, Phys. Rept. 407, 205 (2005).

➤ Presenting the calculation results directly:

C.-Y. Yang and S.-Q. Feng, Phys. Rev. D **112**,036008 (2025)

K meson:
$$M = \frac{2K_6^+}{1 - 2K_6^+ \Pi_{K^0}^{ps}(p)}$$

Where

$$\Pi_{K^0}^{ps}(p_0 = m_{K^0}) = \frac{\beta N_c}{2(2\pi)^2} \sum_{n,s,l} \left(1 + sl \frac{M_d M_s + 2\beta n}{M_{nd} M_{ns}} \right)$$

$$\times \left\{ \int dk_z \frac{1}{E_{dns}} \left[1 - \frac{1}{e^{(E_{dns}-\mu)/T} + 1} - \frac{1}{e^{(E_{dns}+\mu)/T} + 1} \right] + \int dk_z \frac{1}{E_{snl}} \left[1 - \frac{1}{e^{(E_{snl}-\mu)/T} + 1} - \frac{1}{e^{(E_{snl}+\mu)/T} + 1} \right] \right.$$

$$\left. + \left\{ [(M_{nd} - s\kappa_d e_d B) - sl(M_{ns} - l\kappa_s e_s B)]^2 - p_0^2 \right\} B(m_d, m_s) \right\}$$

$$B(m_d, m_s) = \int dk_z \left\{ \frac{1}{E_{dns}} \left[\frac{1}{(E_{dns} + p_0)^2 - E_{snl}^2} \frac{1}{e^{-(E_{dns}+\mu)/T} + 1} - \frac{1}{(E_{dns} - p_0)^2 - E_{snl}^2} \frac{1}{e^{(E_{dns}-\mu)/T} + 1} \right] + \frac{1}{E_{snl}} \left[\frac{1}{(E_{snl} - p_0)^2 - E_{dns}^2} \frac{1}{e^{-(E_{snl}+\mu)/T} + 1} - \frac{1}{(E_{snl} + p_0)^2 - E_{dns}^2} \frac{1}{e^{(E_{snl}-\mu)/T} + 1} \right] \right\}.$$

QCD Phase Diagram Restructuring

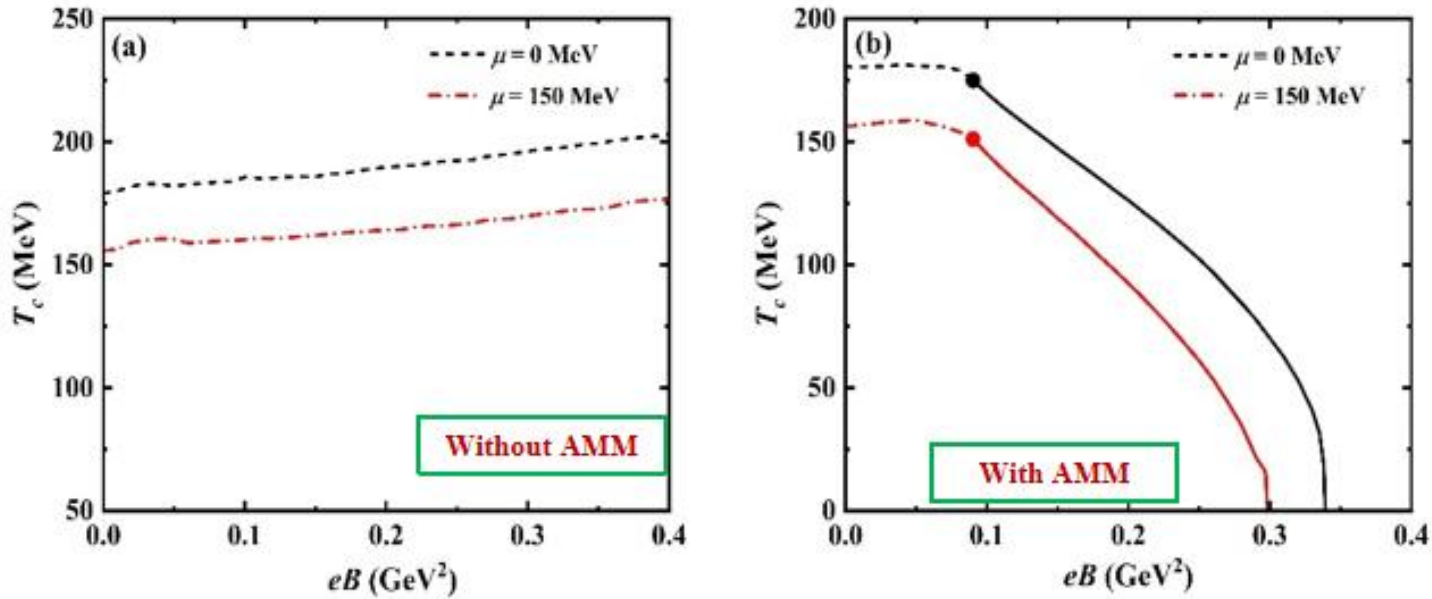


Figure 1 compares the critical temperature (T_c) of chiral phase transitions as a function of eB at different chemical potentials (μ), with and without AMM.

- Magnetic catalysis without AMM
- Inverse magnetic catalysis with AMM
- Non-contradiction with LQCD calculation results.

(1) Phase Diagram Reshaping and CEP Shift: **AMM suppresses T_c and shifts critical endpoints (CEP) toward lower μ and T , contrasting conventional NJL predictions dominated by magnetic catalysis (MC).**

(2) Crossover-to-First-Order Transition: **AMM replaces crossover transitions with first-order transitions under strong eB , validating AMM's role in altering phase transition sequences in multi-flavor systems.**

- (1) C.-Y. Yang and S.-Q. Feng, Phys. Rev. D **112**, 036008 (2025);
- (2) X.-Q. Zhu and S.-Q. Feng, Phys. Rev. D **107**, 016018 (2023);
- (3) Y.-W. Qiu and S.-Q. Feng, X.-Q. Zhu, Phys. Rev. D **108**, 116022 (2023).

The magnetic dependences of neutral pseudoscalar meson mass spectra

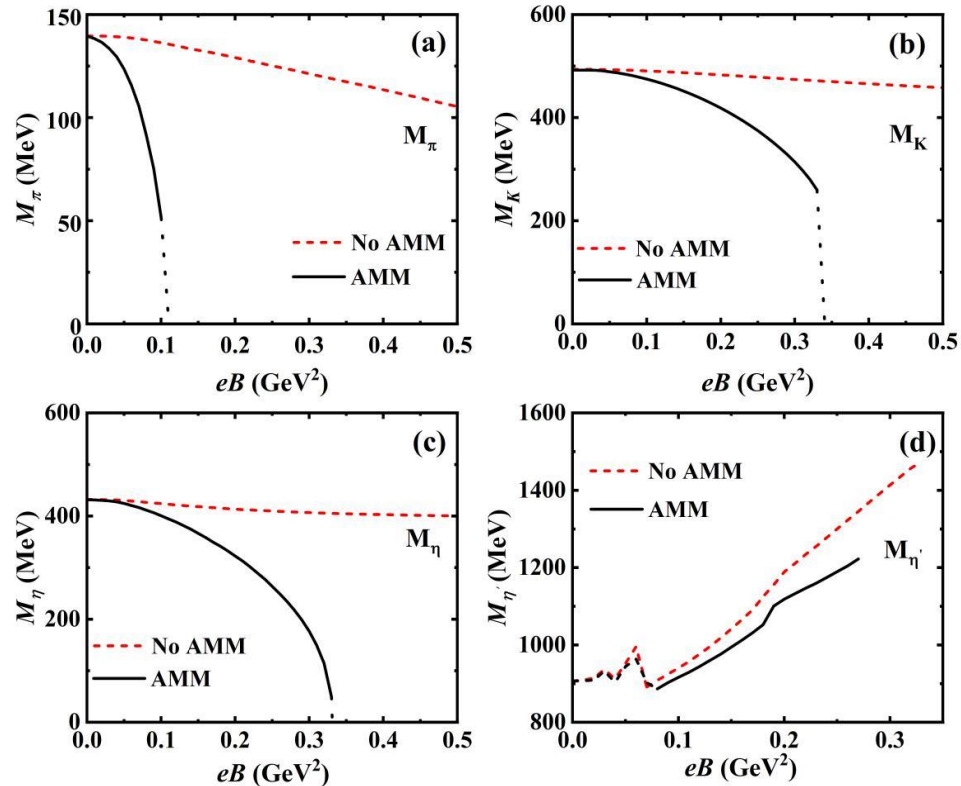


Figure 3 compares the magnetic field dependence of neutral pseudoscalar meson masses (π , K , η , η') at zero temperature, with and without AMM.

- (1) C.-Y. Yang and S.-Q. Feng, Phys. Rev. D **112**, 036008 (2025);
- (2) X.-Q. Zhu and S.-Q. Feng, Phys. Rev. D **107**, 016018 (2023).

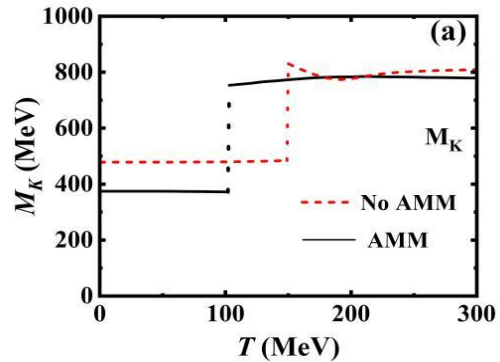
(1) Meson Mass Collapse and Chiral Restoration: AMM triggers abrupt mass collapses (e.g., π at $eB \approx 0.1 \text{ GeV}^2$), directly linking meson stability to chiral symmetry restoration.

(2) η' Resonance Limitations: η' mass diverges under strong eB due to non-perturbative decay width effects, exposing NJL's limitations in handling resonance states.

Key Issues Addressed:

Systematically reveals AMM's role in regulating multi-flavor meson masses and flavor mixing (e.g., π^0 - η - η'), addressing gaps in two-flavor models' predictions for magnetic sensitivity.

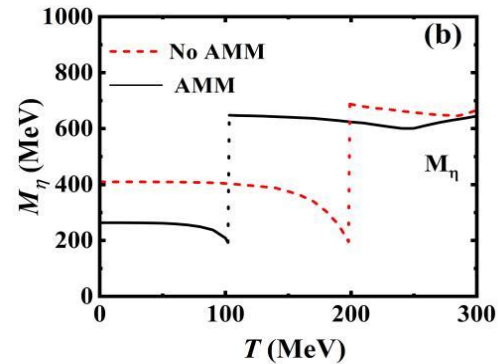
The temperature dependences of neutral pseudoscalar meson masses



● K meson: $T_{mott} \approx 149 \text{ MeV} < T_c \approx 192 \text{ MeV}$ without AMM

$T_{mott} = T_c \approx 102 \text{ MeV}$ with AMM

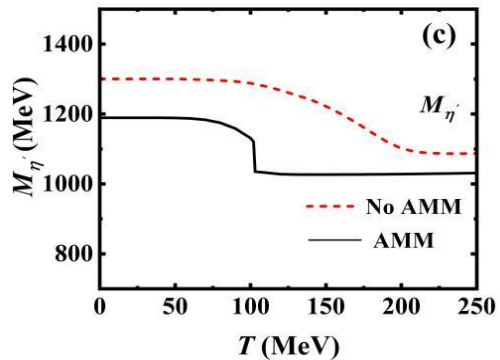
T_{mott} with AMM $< T_{mott}$ without AMM



● η meson: $T_{mott} \approx 198 \text{ MeV} > T_c \approx 192 \text{ MeV}$ without AMM

$T_{mott} = T_c \approx 102 \text{ MeV}$ with AMM

T_{mott} with AMM $< T_{mott}$ without AMM



● η' meson: The fastest decline in mass without AMM at $T = 179 \text{ MeV}$

The fastest decline in mass with AMM at $T = 102 \text{ MeV}$

Key Issues Addressed:

Demonstrates how AMM-driven quark mass dynamics reshape meson transition pathways, resolving uncertainties in predicting meson stability under high T and B .

(1) C.-Y. Yang and S.-Q. Feng, Phys. Rev. D **112**, 036008 (2025);

(1) X.-Q. Zhu and S.-Q. Feng, Phys. Rev. D **107**, 016018 (2023).

The 26th international symposium on spin physics (SPIN2025), Qingdao, Sept. 21 - 26, 2025

3. Summary and Conclusions

The 26th international symposium on spin physics (SPIN2025) , Qingdao, Sept. 21 - 26, 2025

Summary and conclusions

1. The spin alignment of ρ_{00} and phase structure of thermal QGP under rotation are investigated. It is found that **chiral imbalance have some effects on phase structure of QGP medium. We also study some dependences of spin alignment of ρ_{00} with temperature, angular velocity, rotational radius on chiral imbalance.**

2. The research investigates **the impact of the anomalous magnetic moment (AMM) of quarks on the mass spectra of neutral pseudoscalar mesons (π, K, η, η') under conditions of strong magnetic fields, finite temperatures, and chemical potentials, based on the three-flavor Nambu-Jona-Lasinio (NJL) model.**

Thanks !

The 26th international symposium on spin physics (SPIN2025) , Qingdao, Sept. 21 - 26, 2025